

Structure of the Ebola VP35 interferon inhibitory domain

Daisy W. Leung^a, Nathaniel D. Ginder^a, D. Bruce Fulton^a, Jay Nix^b, Christopher F. Basler^c, Richard B. Honzatko^a, and Gaya K. Amarasinghe^{a,1}

^aDepartment of Biochemistry, Biophysics and Molecular Biology, Iowa State University, Ames, IA 50011; ^bAdvanced Light Source, Lawrence Berkeley National Laboratory, Berkeley, CA 94720; and ^cDepartment of Microbiology, Mount Sinai School of Medicine, New York, NY 10029

Edited by Ian A. Wilson, The Scripps Research Institute, La Jolla, CA, and accepted by the Editorial Board November 22, 2008 (received for review August 8, 2008)

Ebola viruses (EBOVs) cause rare but highly fatal outbreaks of viral hemorrhagic fever in humans, and approved treatments for these infections are currently lacking. The Ebola VP35 protein is multifunctional, acting as a component of the viral RNA polymerase complex, a viral assembly factor, and an inhibitor of host interferon (IFN) production. Mutation of select basic residues within the C-terminal half of VP35 abrogates its dsRNA-binding activity, impairs VP35-mediated IFN antagonism, and attenuates EBOV growth in vitro and in vivo. Because VP35 contributes to viral escape from host innate immunity and is required for EBOV virulence, understanding the structural basis for VP35 dsRNA binding, which correlates with suppression of IFN activity, is of high importance. Here, we report the structure of the C-terminal VP35 IFN inhibitory domain (IID) solved to a resolution of 1.4 Å and show that VP35 IID forms a unique fold. In the structure, we identify 2 basic residue clusters, one of which is important for dsRNA binding. The dsRNA binding cluster is centered on Arg-312, a highly conserved residue required for IFN inhibition. Mutation of residues within this cluster significantly changes the surface electrostatic potential and diminishes dsRNA binding activity. The high-resolution structure and the identification of the conserved dsRNA binding residue cluster provide opportunities for antiviral therapeutic design. Our results suggest a structure-based model for dsRNA-mediated innate immune antagonism by Ebola VP35 and other similarly constructed viral antagonists.

crystal structure | Ebola virus | RNA binding

Ebola viruses (EBOVs) cause severe hemorrhagic fever characterized by fever, shock, coagulation defects, and impaired immunity (1, 2). These manifestations of infection are thought to reflect subversion of the innate immune system coupled with uncontrolled viral replication, particularly in macrophages and dendritic cells (3, 4). EBOV infection of these cells enhances production of proinflammatory cytokines, such as TNF- α and IFN (IFN)- γ , and diminishes stimulation of T cell maturation by dendritic cells (3, 4). Like other negative-strand RNA viruses that impair both innate and adaptive immunity (e.g., influenza, rabies, and measles), EBOV suppresses host IFN activities to replicate, thus resulting in serious disease (5, 6). Only individuals who survive EBOV infection show appreciable amounts of viral-specific antibodies (7), suggesting that EBOV infections lead to shutdown of early immune responses and prevent activation of adaptive immune responses.

Recognition of viral particles and viral RNA, including RNA modifications such as 5'-triphosphate (5'-ppp), by cytosolic pattern recognition receptor helicases RIG-I and MDA-5 leads to activation of transcription factors, including IFN regulatory factor-3 (IRF-3), IRF-7, NF- κ B, and AP-1 (8–12). These transcription factors in turn induce expression of a large number of cytokines, such as IFN- α and IFN- β (13). Activated IFN genes operate in both autocrine and paracrine manners to stimulate the activity of additional antiviral genes. Therefore, inhibition of signaling mechanisms that promote IFN responses is a necessary

viral countermeasure against the host antiviral system and critical for viral propagation (2).

Ebola viral protein 35 (VP35) is multifunctional, serving as a component of the viral RNA polymerase complex, as a structural/assembly factor, and as a suppressor of host IFN responses (2). Therefore, a functional VP35 is required for efficient viral replication and pathogenesis; knockdown of VP35 leads to reduced viral amplification and reduced lethality in infected mice (14–18). However, limited information is available regarding how VP35 is able to perform multiple functions. VP35 contains an N-terminal coiled-coil domain required for its oligomerization (19, 20) and a C-terminal dsRNA-binding region (15, 16, 21). Oligomerization through the N-terminal oligomerization domain is required for virus replication because oligomerization-defective mutants fail to interact with the viral polymerase (L) protein (15, 22). Similarly, deletion of the N-terminal region or mutation of the coiled-coil domain abrogates IFN suppression by VP35, which can be overcome by tethering a heterologous oligomerization module to the VP35 C terminus or overexpression of the isolated VP35 C terminus (20). The latter observations suggest a model where the coiled-coil domain provides a critical oligomerization function, whereas the C-terminal region of VP35 interacts with host factors to block signaling that triggers IFN responses.

The host factor(s) directly targeted by VP35 have not been definitively identified. Only VP35, and not any other Ebola protein, supports viral growth of a mutant influenza A virus that lacks the IFN suppressor protein NS1A, suggesting that VP35 also inhibits IFN activity (23). A bioinformatics study identified an 8-residue motif in VP35 that has 75% sequence identity to the influenza NS1A protein, including basic residues essential for binding of dsRNA by NS1 (21). Mutation of these residues impaired NS1A inhibition of IFN responses (24). Based on this identity, it was suggested that this motif could also be required for inhibition of IFN responses by VP35 (21). Consistent with these observations, VP35 inhibits phosphorylation, activation, and nuclear localization of IRF-3 and inhibits viral- and dsRNA-induced expression of the IFN β gene (14, 17, 18, 21, 25, 26). VP35 also inhibits activation of the cellular antiviral kinase RNA-dependent protein kinase (PKR) (16) and activation of the RNAi pathway (27). These pathways are similarly targeted by

Author contributions: D.W.L. and G.K.A. designed research; D.W.L., D.B.F., J.N., and G.K.A. performed research; C.F.B. contributed new reagents/analytic tools; D.W.L., N.D.G., R.B.H., and G.K.A. analyzed data; and D.W.L., C.F.B., and G.K.A. wrote the paper.

The authors declare no conflict of interest.

This article is a PNAS Direct Submission. I.A.W. is a guest editor invited by the Editorial Board.

Data deposition: The atomic coordinates have been deposited in the Protein Data Bank, www.pdb.org (PDB ID: 3FKE).

¹To whom correspondence should be addressed. E-mail: amarasin@iastate.edu.

This article contains supporting information online at www.pnas.org/cgi/content/full/0807854106/DCSupplemental.

© 2009 by The National Academy of Sciences of the USA

other virus-encoded dsRNA-binding proteins. Examples include the influenza virus NS1A protein, the reovirus $\sigma 3$ protein (28), and the vaccinia virus E3L protein (29), which can inhibit host antiviral responses through dsRNA-dependent and -independent mechanisms.

The mechanism by which VP35 inhibits IRF-3 activation and IFN α/β expression is not completely understood, but thus far, VP35 IFN-antagonist function correlates with VP35 dsRNA binding activity. EBOV likely activates the RIG-I pathway (15, 25) and VP35 expression inhibits the RIG-I activated signaling pathway (15). Because coexpression of VP35 can inhibit activation of IFN β gene expression by overexpressed IKK ϵ or TBK-1, it appears that VP35 may target these kinases to exert its inhibitory effect, although additional mechanisms directed at more upstream points in these pathways cannot be excluded. Indeed, mutation of basic residues such as Arg-312 to alanine (Arg312Ala) severely impairs VP35 dsRNA binding and IFN-antagonist activity, but does not significantly affect VP35 function as part of the viral polymerase complex (15, 17, 21, 25). Viruses containing the Arg312Ala mutation more readily activate IRF-3, compared with a wild-type virus, and induce a much stronger innate immune response than wild-type virus. Taken together, these data correlate dsRNA binding with the inability of the Arg312Ala mutant virus to support viral growth because of aberrant IFN inhibition (22, 25). Strikingly, an Arg312Ala VP35 mutant EBOV is greatly attenuated relative to the wild-type virus in mice (25).

These data suggest that the dsRNA binding activity mediated by the C terminus of VP35 is critical for viral suppression of innate immunity and for virulence (14, 25). Yet, the structure of the VP35 C terminus has not been available, and it is not clear how individual mutations impair dsRNA binding and suppress innate immune signaling. As an initial step toward addressing these questions, we conducted a structural and biochemical analysis of the C-terminal region of Ebola VP35. Here, we report the 3-dimensional structure of the VP35 IFN inhibitory domain (IID) solved by X-ray crystallography and identify residues important for RNA binding. Our structure reveals a unique fold that binds dsRNA. Examination of the VP35 IID structure reveals 2 basic patches that are highly conserved among members of the *Filoviridae* family (identical among EBOV isolates). Biochemical and NMR-based structural analyses show that one patch contains residues that are required for dsRNA binding and IFN inhibition, whereas the functional significance of the other basic patch remains unknown. Although the structure of VP35 IID is significantly different from that of influenza NS1A RNA-binding domain (RBD), the basic side chains at the dimer interface of the NS1A RBD and those located near Arg-312 in VP35 IID are positioned to form contiguous basic patches, suggesting that NS1A and VP35 may interact with dsRNA in a similar manner. Our results provide structural insights into the role of conserved residues in dsRNA binding that are required for full EBOV virulence and suggest a model for RNA-dependent Ebola VP35 functions.

Results

Crystal Structure of EBOV VP35 Was Solved to High Resolution. Using NMR-based studies, we identified the minimal structured region from the C terminus of Ebola VP35 IID and the crystal structure of VP35 IID was solved to 1.4-Å resolution (Fig. 1*B* and *C*). In the crystal, there are 2 nearly identical monomers (A and B) of VP35 IID in the asymmetric unit [supporting information (SI) Text, Table S1, and Fig. S1]. PROCHECK analysis revealed that 95.2% of the residues are located in the most -favored regions (A, B, L) of the Ramachandran plot, whereas the remaining 4.8% are in the additional allowed regions (a, b, l, p). No electron density is observed for the first 4 residues from monomer A and the first 2 residues from monomer B. Previous studies have

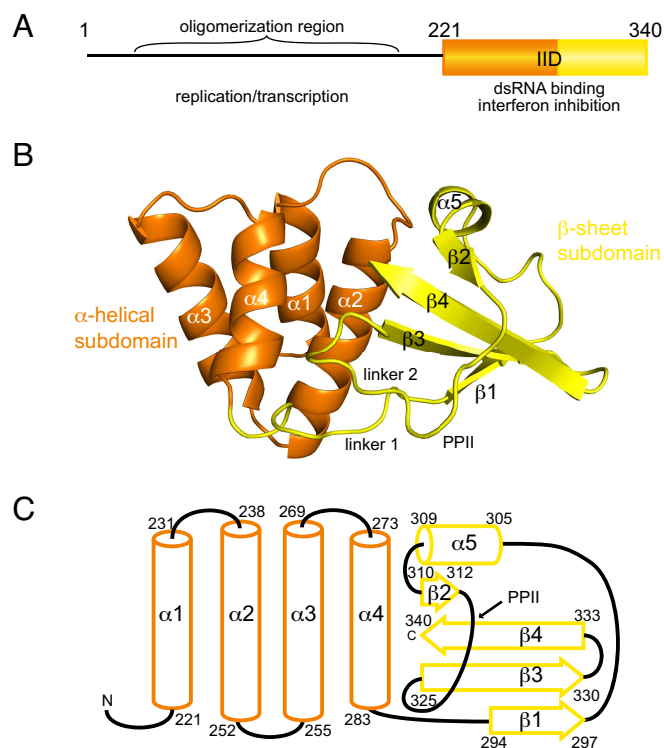
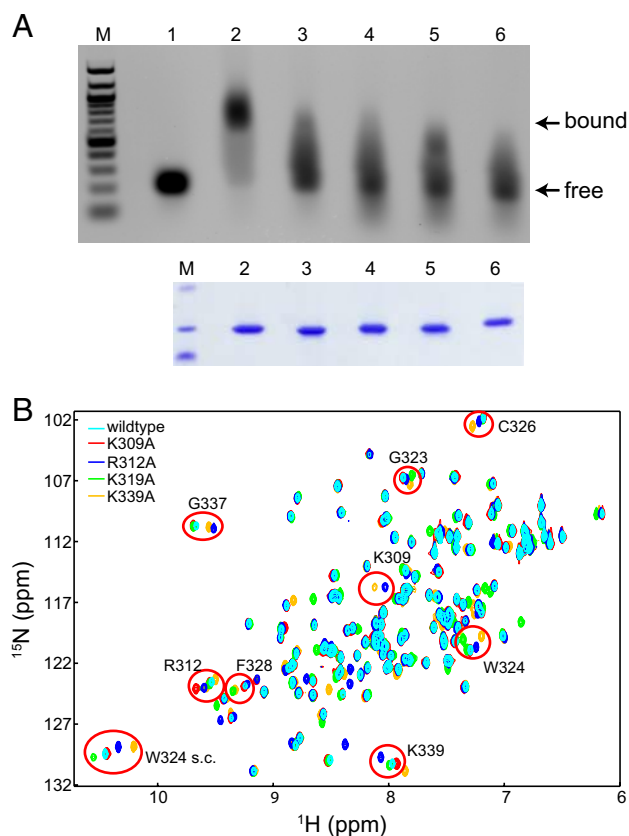


Fig. 1. Crystal structure of VP35 C-terminal IFN-inhibitory domain (IID) reveals a fold that binds dsRNA. (A) Domain organization of VP35. (B) Ribbon representation of VP35 IID. Secondary structural elements that form the α -helical subdomain (orange) and the β -sheet subdomain (yellow). (C) Topology and delimiting sequence markers of VP35 IID.

shown that full-length VP35 forms oligomers through the N-terminal oligomerization region. However, both dynamic light-scattering and analytical ultracentrifugation experiments demonstrate that VP35 IID is monomeric in solution (Fig. S2). Furthermore, the buried surface area between monomer A and monomer B in the asymmetric unit is ≈ 490 Å², indicating that the interaction between the monomers observed in the VP35 IID crystal is weak at best.

VP35 IID Comprises 2 Subdomains. The VP35 IID structure is organized into 2 subdomains: an N-terminal α -helical subdomain and a C-terminal β -sheet subdomain (Fig. 1*B* and *C*). The α -helical subdomain (residues 221–283) is a 4-helical bundle ($\alpha 1$ – $\alpha 4$), arranged in 2 layers, with $\alpha 1$ and $\alpha 2$ helices packed against $\alpha 3$ and $\alpha 4$ helices to form the core of the α -helical subdomain. The $\alpha 2$ and $\alpha 4$ helices pack against the β -sheet subdomain. The β -sheet subdomain (residues 294–340) is composed of a 4-stranded mixed β -sheet ($\beta 1$ – $\beta 4$) and a short helical segment, $\alpha 5$. The $\beta 1$ strand connects to $\alpha 5$ helix through a long linker that includes a reverse turn. The $\alpha 5$ helix leads into a hairpin turn, followed by the short $\beta 2$ strand and the longer $\beta 3$ and $\beta 4$ strands. The $\beta 2$ – $\beta 4$ strands are antiparallel whereas the $\beta 1$ strand is parallel to the $\beta 3$ strand (Fig. 1*B*). Linker 1, which includes Pro-292 and Pro-293 residues, connects the subdomains. Residues between the $\beta 2$ and $\beta 3$ strands of VP35 IID (linker 2 and Pro-313 to Pro-318) form a left-handed polyproline Type II helix (PPII), a feature that is not characteristic of canonical dsRNA-binding domains (dsRBDs). The PPII helix packs against the $\beta 3$ strand and the Type I hairpin loop formed by residues Lys-319 to Gly-323.

VP35 IID Forms a Unique Fold. The overall structure of VP35 IID represents a unique fold for a dsRBD that is substantially



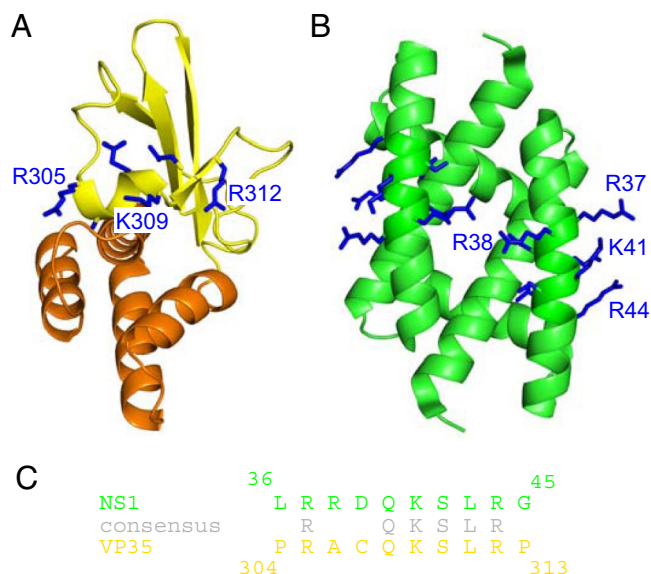


Fig. 5. The RNA-binding domains of Ebola VP35 and influenza NS1 proteins are incorporated into distinct scaffolds. (A and B) Structures of the Ebola VP35 IID (this study; left) (A) and the influenza NS1A dsRNA binding domain (PDB ID code 2ZKO) (B). (C) Similar side chains of arginine and lysine residues in the 8-residue alignment between the NS1A and VP35 protein sequences are shown and highlighted in gray (adapted from ref. 21).

β 2 strand, which in influenza NS1A is incorporated entirely within a single helix (31). NS1 proteins form obligatory dimers, which require contacts from the RNA-binding domain. In contrast, VP35 forms trimers through contacts at the N terminus (ref. 20 and D.W.L. and G.K.A., unpublished observations) that are independent of the dsRNA-binding domain. Moreover, isolated VP35 IID protein is monomeric in solution, even at high concentrations (Fig. S2). Despite these differences, the basic residue side chains, which are important for RNA binding, form similar contiguous patches (Fig. 5A and B) (21). Altogether, this data along with the ability of influenza NS1 and Ebola VP35 to mutually substitute IFN-suppressive functions suggest that these 2 proteins may target similar components in the host immune system. However, differences we observe between VP35 and NS1 proteins in their overall structures, oligomeric states, and the structural requirements for oligomerization, may reflect additional functionalities performed by these proteins that further contribute to the high virulence displayed by Ebola and influenza viruses.

Recent studies also show that EBOV can activate antiviral pathways that operate through RIG-I and MDA-5 to activate IFN regulatory factor 3 (IRF-3) (15, 25) and that Ebola VP35 protein can inhibit these antiviral responses (15). Cardenas *et al.* showed that VP35 may directly interact with host proteins at points proximal to IRF-3, possibly interacting with and preventing the activation or function of the kinases IKK ϵ and TBK-1, which phosphorylate and activate IRF-3 (15). Furthermore, VP35 mutants that are unable to bind dsRNA also show reduced but appreciable suppression of IRF-3 phosphorylation and nuclear localization (15, 22), suggesting that IFN-inhibitory activity of VP35 involves multiple modes. Our structure reveals that residues critical for dsRNA binding and immune inhibition form an extended basic patch. Mutation of these residues results in only minor structural perturbations, yet prevents interactions with dsRNA. Based on these observations, we now propose a model, shown in Fig. 6, where VP35 suppresses IRF-3 activation by dsRNA-dependent activity through direct sequestration of dsRNA and through inhibition of the RIG-I/MDA-5 helicases.

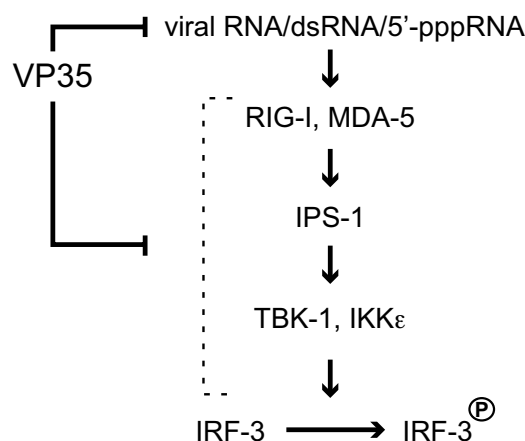


Fig. 6. Model for VP35-mediated IFN inhibition and immune suppression.

Recent structural and biochemical analyses of RIG-I and PKR, an RNA-dependent protein kinase, revealed that additional modifications such as 5' triphosphate groups can play a role in the RNA recognition by RIG-I to provide additional specificity (11, 12). Alternatively, VP35 can suppress host immune responses through dsRNA-independent activity perhaps by direct binding and inhibition of IRF-3 kinases (15). Our current study suggests that both activities are likely to be mediated through mechanisms that involve interactions with the conserved basic patch centered on Arg-312 and therefore, any changes to residues located on this patch can lead to reduced host immune evasion. Consistent with our model, a recent microarray analysis showed that a recombinant EBOV containing an Arg312Ala mutation leads to activation of antiviral responses, whereas the wild-type virus completely shuts down host innate immune signaling (25). Together, these studies suggest that the conserved basic patch identified in our study can mediate multiple IFN inhibitory mechanisms and is critical for viral replication and pathogenesis.

Emerging and reemerging viruses such as Ebola are a significant threat to global human health, and the critical role played by Ebola VP35 in host immune suppression is well established. Our crystal structure of VP35 IID now provides a framework to understand structural characteristics that promote interactions between VP35 and dsRNA, which correlates with the ability of Ebola VP35 to antagonize host antiviral signaling pathways. High sequence conservation among filoviruses suggests that VP35 proteins from other family members will likely retain similar architecture. High-resolution structure and solution-state NMR data from this study provide opportunities for targeted antiviral and diagnostic drug design. The unique information afforded by the structure of Ebola VP35 IID will also facilitate future studies to reveal regulatory mechanisms at a key host-viral interface.

Methods

Crystallization and Diffraction Data Collection. Initial conditions for crystallization were identified by using purified VP35 IID protein (SI Text) and a commercial screen (Hampton Research). In-house optimized native and selenomethionine crystals were grown at 25 °C by the hanging-drop vapor-diffusion method with 17 mg/ml protein solutions diluted with 200 mM sodium citrate (pH 5.8) and 11% (wt/vol) PEG 4000. Crystals were soaked in reservoir solution with 25% glycerol (wt/vol) and frozen in a nitrogen stream. Diffraction data were collected at the Advanced Light Source (beamline 4.2.2) at 100 K (statistics are listed in Table S1).

Structure Determination and Refinement. Data were processed by using d*TREK (33). Intensities were converted to structure factors by using the CCP4 program TRUNCATE (34). Phases were determined from a multiple-

wavelength anomalous dispersion (MAD) experiment performed on a Se-Met substituted crystal. Phasing was performed with the SOLVE/RESOLVE program package (35). ARP/wARP (36) was used to trace the backbone by using the VP35 sequence, which led to an initial model with $\approx 20\%$ of the residues modeled as alanine. The rest of the model was constructed manually by using XtalView (37) into an electron density map generated from MAD phases to 1.4-Å resolution by using native data. Refinement was performed against the structure factors by using CNS (38) and REFMAC5 (39). Refinement included simulated annealing, followed by conjugate gradient energy minimization. Individual thermal parameters were refined after each cycle of simulated annealing and subject to standard restraints. Water molecules were automatically added by using CNS if a peak $>3.0\sigma$ was present in Fourier maps with coefficients ($F_{\text{obs}} - F_{\text{calc}}\rangle e^{i\alpha_{\text{calc}}}$). The contribution of bulk solvent to structure factors was determined by CNS (default parameters). The model was further

refined by using REFMAC5 using MLKF residual function, weight matrix of 0.75, bulk solvent scaling, and individual anisotropic B-factors. The refined model was verified by using a $2F_o - F_c$ map showing that all residues have continuous electron density. Final refinement statistics are shown in Table S1.

ACKNOWLEDGMENTS. We thank Drs. R. DeGuzman, D. Klein, and D. Borek for support and discussions; Dr. M. Shogren-Knaak, Dr. M. Nilsen-Hamilton, Dr. T. Bobik, H. Azzaz, C. Warner, and S. Kakar for helpful discussions; the ISU X-ray Crystallography facility and Dr. J. Hoy for assistance with initial X-ray data collection; Dr. D. Klein for providing the dsRNA; and P. Ramanan, L. Helgeson, D. Peterson, and M. Farahbakhsh for laboratory assistance. This work was supported in part by the Roy J. Carver Charitable Trust Grant 09-3271 (to G.K.A.), a Roy J. Carver Trust Graduate Fellowship (to N.D.G.), and National Institutes of Health Grant AI059536 (to C.F.B.).

- Sanchez A, Geisbert TW, Feldmann H (2006) Filoviridae: Marburg and Ebola Viruses. *Fields Virology*, eds Knipe DM, et al. (Lippincott Williams & Wilkins, Philadelphia), 5th Ed, pp 1409–1448.
- Zampieri CA, Sullivan NJ, Nabel GJ (2007) Immunopathology of highly virulent pathogens: Insights from Ebola virus. *Nat Immunol* 8:1159–1164.
- Bosio CM, et al. (2003) Ebola and Marburg viruses replicate in monocyte-derived dendritic cells without inducing the production of cytokines and full maturation. *J Infect Dis* 188:1630–1638.
- Mahanty S, et al. (2003) Protection from lethal infection is determined by innate immune responses in a mouse model of Ebola virus infection. *Virology* 312:415–424.
- Bray M, Geisbert TW (2005) Ebola virus: The role of macrophages and dendritic cells in the pathogenesis of Ebola hemorrhagic fever. *Int J Biochem Cell Biol* 37:1560–1566.
- Bray M, Mahanty S (2003) Ebola hemorrhagic fever and septic shock. *J Infect Dis* 188:1613–1617.
- Baize S, et al. (1999) Defective humoral responses and extensive intravascular apoptosis are associated with fatal outcome in Ebola virus-infected patients. *Nat Med* 5:423–426.
- Saito T, Gale M, Jr (2007) Principles of intracellular viral recognition. *Curr Opin Immunol* 19:17–23.
- Thompson AJ, Locarnini SA (2007) Toll-like receptors, RIG-I-like RNA helicases and the antiviral innate immune response. *Immunol Cell Biol* 85:435–445.
- Tortorella D, Gewurz BE, Furman MH, Schust DJ, Ploegh HL (2000) Viral subversion of the immune system. *Annu Rev Immunol* 18:861–926.
- Cui S, et al. (2008) The C-terminal regulatory domain is the RNA 5'-triphosphate sensor of RIG-I. *Mol Cell* 29:169–179.
- Marques JT, et al. (2006) A structural basis for discriminating between self and nonself double-stranded RNAs in mammalian cells. *Nat Biotechnol* 24:559–565.
- Basler CF, Garcia-Sastre A (2002) Viruses and the type I interferon antiviral system: Induction and evasion. *Int Rev Immunol* 21:305–337.
- Basler CF, et al. (2003) The Ebola virus VP35 protein inhibits activation of interferon regulatory factor 3. *J Virol* 77:7945–7956.
- Cardenas WB, et al. (2006) Ebola virus VP35 protein binds double-stranded RNA and inhibits alpha/beta interferon production induced by RIG-I signaling. *J Virol* 80:5168–5178.
- Feng Z, Cervený M, Yan Z, He B (2007) The VP35 protein of Ebola virus inhibits the antiviral effect mediated by double-stranded RNA-dependent protein kinase PKR. *J Virol* 81:182–192.
- Hartman AL, et al. (2008) Inhibition of IRF-3 activation by VP35 is critical for the high level of virulence of Ebola virus. *J Virol* 82:2699–2704.
- Enterlein S, et al. (2006) VP35 knockdown inhibits Ebola virus amplification and protects against lethal infection in mice. *Antimicrob Agents Chemother* 50:984–993.
- Moller P, Pariente N, Klenk HD, Becker S (2005) Homo-oligomerization of Marburgvirus VP35 is essential for its function in replication and transcription. *J Virol* 79:14876–14886.
- Reid SP, Cardenas WB, Basler CF (2005) Homo-oligomerization facilitates the interferon-antagonist activity of the ebolavirus VP35 protein. *Virology* 341:179–189.
- Hartman AL, Townner JS, Nichol ST (2004) A C-terminal basic amino acid motif of Zaire ebolavirus VP35 is essential for type I interferon antagonism and displays high identity with the RNA-binding domain of another interferon antagonist, the NS1 protein of influenza A virus. *Virology* 328:177–184.
- Hartman AL, Dover JE, Townner JS, Nichol ST (2006) Reverse genetic generation of recombinant Zaire Ebola viruses containing disrupted IRF-3 inhibitory domains results in attenuated virus growth in vitro and higher levels of IRF-3 activation without inhibiting viral transcription or replication. *J Virol* 80:6430–6440.
- Basler CF, et al. (2000) The Ebola virus VP35 protein functions as a type I IFN antagonist. *Proc Natl Acad Sci USA* 97:12289–12294.
- Donelan NR, Basler CF, Garcia-Sastre A (2003) A recombinant influenza A virus expressing an RNA-binding-defective NS1 protein induces high levels of beta interferon and is attenuated in mice. *J Virol* 77:13257–13266.
- Hartman AL, Ling L, Nichol ST, Hibberd ML (2008) Whole-genome expression profiling reveals that inhibition of host innate immune response pathways by Ebola virus can be reversed by a single amino acid change in the VP35 protein. *J Virol* 82:5348–5358.
- Gupta M, Mahanty S, Ahmed R, Rollin PE (2001) Monocyte-derived human macrophages and peripheral blood mononuclear cells infected with Ebola virus secrete MIP-1alpha and TNF-alpha and inhibit poly-IC-induced IFN-alpha in vitro. *Virology* 284:20–25.
- Haasnoot J, et al. (2007) The Ebola virus VP35 protein is a suppressor of RNA silencing. *PLoS Pathog* 3:e86.
- Imani F, Jacobs BL (1988) Inhibitory activity for the interferon-induced protein kinase is associated with the reovirus serotype 1 sigma 3 protein. *Proc Natl Acad Sci USA* 85:7887–7891.
- Chang HW, Jacobs BL (1993) Identification of a conserved motif that is necessary for binding of the Vaccinia virus E3L gene products to double-stranded RNA. *Virology* 194:537–547.
- Johnson RF, McCarthy SE, Godlewski PJ, Harty RN (2006) Ebola virus VP35–VP40 interaction is sufficient for packaging 3E–5E minigenome RNA into virus-like particles. *J Virol* 80:5135–5144.
- Chien CY, et al. (2004) Biophysical characterization of the complex between double-stranded RNA and the N-terminal domain of the NS1 protein from influenza A virus: Evidence for a novel RNA-binding mode. *Biochemistry* 43:1950–1962.
- Yin C, et al. (2007) Conserved surface features form the double-stranded RNA binding site of non-structural protein 1 (NS1) from influenza A and B viruses. *J Biol Chem* 282:20584–20592.
- Pflugrath JW (1999) The finer things in X-ray diffraction data collection. *Acta Crystallogr D* 55(Pt 10):1718–1725.
- Collaborative Computational Project N (1994) The CCP4 suite: Programs for protein crystallography. *Acta Crystallogr D* 50:760–763.
- Terwilliger TC, Berendzen J (1999) Automated MAD and MIR structure solution. *Acta Crystallogr D* 55(Pt 4):849–861.
- Perrakis A, Sixma TK, Wilson KS, Lamzin VS (1997) wARP: Improvement and extension of crystallographic phases by weighted averaging of multiple-refined dummy atomic models. *Acta Crystallogr D* 53(Pt 4):448–455.
- McRee DE (1999) XtalView/Xfit—A versatile program for manipulating atomic coordinates and electron density. *J Struct Biol* 125:156–165.
- Brunger AT, et al. (1998) Crystallography NMR system: A new software suite for macromolecular structure determination. *Acta Crystallogr D* 54(Pt 5):905–921.
- Murshudov GN, Vagin AA, Dodson EJ (1997) Refinement of macromolecular structures by the maximum-likelihood method. *Acta Crystallogr D* 53(Pt 3):240–255.